Mechanisms Controlling Leaching Kinetics of Fixated Flue Gas Desulfurization (FGD) Material: the pH Effect

C. M. Cheng and Harold Walker

The Ohio State University, Department of Civil and Environmental Engineering and Geodetic Science, 470 Hitchcock Hall, 2070 Neil Ave.
Columbus, Ohio 43210

KEYWORDS: fixated FGD material, leaching, kinetics, pH effect.

ABSTRACT

A flow-through-rotating-disk system was applied to study the pH effect on the leaching kinetics of fixated FGD material. The objectives of this study were (1) to determine if the leaching kinetics are surface- or transport-controlled, (2) to elucidate the role of pH in controlling the leaching kinetics, and (3) to propose pH-dependent leaching models for specific elements. The independence of leaching rates of selected elements on various hydrodynamic conditions indicated a surface-controlled reaction mechanism. The leaching rates of major and minor elements including Ca, S, Al, Si, Mg, and Fe all increased with decreasing pH. Leaching rates of divalent and trivalent cations at acidic leaching conditions increased 3.2 and 5.2 times, respectively, as pH decreased 1 unit.

INTRODUCTION

Approximately 20 million metric tons of fixated FGD material is produced every year in the United States. The alkali and cementitious properties of fixated FGD material [1,2,3] suggest that it can be beneficially used in agricultural and engineering applications. Numerous studies have been carried out to increase beneficial utilization; e.g., acid soil amendment [4,5,6,7,8], acid mine drainage sealing [9,10,11], and engineering materials [12,13,14,15]. However, the release of heavy metals from this material potentially results in adverse environmental impacts [4,7,8,11,14].

Many leaching studies have been conducted to understand the release potential of heavy metals from fly ash under various leaching environments at either equilibrium or near-equilibrium conditions. However, these results depend highly on the leaching conditions, and therefore, provide no general view [16] and cannot be applied to predict field leachate concentrations [17]. In addition, very few studies have examined the kinetics of the leaching process. Thus, there is a lack of fundamental knowledge about the mechanisms affecting the leaching behavior of this material.

To develop a better understanding of the leaching behavior of fixated FGD material, this research (1) determined whether the leaching kinetics of specific elements from fixated FGD material are transport- or reaction-controlled, (2) elucidated the role of pH on controlling the leaching kinetics of fixated FGD material, and (3) proposed pH-dependent leaching models for specific elements.

EXPERIMENTAL

The fixated FGD material used in this study was manufactured by mixing FGD material (filter cake, FC) and fly ash (FA) from a coal-fired power plant near Conesville, Ohio, with a FA/FC ratio of 1.5/1 (dry weight basis). Milli-Q water and an additional 6% quicklime were added to produce a final mixture with 30% moisture content. The mixture was then compacted in the shape of a disk with dimensions of 3.18 cm and 0.8cm in diameter and thickness, respectively, and then cured in a 100-% humidity room. After curing for 28 days, the fixated FGD material disk was oven-dried at 60^{o}C over night and then stored in a vacuum desiccator containing diphosphorus pentoxide (P_2O_5) to terminate the hydration process. Leachant solution was prepared by adding sodium nitrate into Milli-Q water to a final concentration of 0.01 M. Complete elemental analysis of fixated FGD material was accomplished according to EPA method 3052.

Leaching experiments were carried out in a flow-through-rotating-disk system. This system was chosen because (1) the flux of reagents (e.g., protons) to the FGD by-product surface can be conveniently controlled by changing the rotation speed of the disk; (2) an exact solution to the Navier-Stokes equation describing the hydrodynamics of this system exists; and thus (3) allowing for the precise prediction of transport-controlled rates of reactants and products, to and from, the disk surface. In this system, a fixated FGD material disk was attached to a Teflon-lined rotator with an acrylic sample holder. Temperature was controlled by a thermo-regulated water bath at 25.0$\pm$0.1^{o}C. The pH in the reactor was adjusted by a pH-stat autotitrator with trace-metal grade nitric acid with the relative standard deviation of less than 1%. The rotating speed of the disk was controlled by a motorized mixer.

In each leaching experiment, a constant pH and disk rotating speed was maintained. Five different acidic leaching conditions ranging from pH 2.2 to 6.8 were tested. A rotating speed of 60 rpm was applied to each acidic leaching condition. Other rotating speeds were also carried out at pH 2.2 and 5.0. The surface roughness of fixated FGD material disk was kept constant by polishing the surface with 320 grit waterproof silicon carbide paper before every experiment began. Samples were collected periodically until the leaching process reached steady state (i.e., the relative standard deviation of element concentrations from the last four successive effluent samples was less than 10%).

Inductively Coupled Plasma-Optical Emission Spectrometry (ICP-OES) was applied to analyze major and minor elements; i.e., Al, Ca, Fe, S, Si, and Mg. The

specific surface area of each disk was characterized by the BET technique. The change of mineral phases and morphology on the surface of the fixated FGD material disk before and after leaching were studied with X-ray diffraction (XRD) and scanning electronic microscopy (SEM).

The experimentally determined leaching rate (e.g., μmole cm^{-2} min^{-1}) of a selected element i is calculated as:

$$R_i = \frac{\overline{C}_{i,eff} \times \overline{Q}}{A} \tag{1}$$

where $\overline{C}_{i,eff}$ is the mean concentration value of the last four successive samples collected after steady state is reached (e.g., μmole L^{-1}), $\overline{Q}$ is the average value of the last four measurements of the flow rates (e.g., L min^{-1}), and A is total surface area of fixated FGD material after leaching (e.g., cm^2). The error in the calculated rate was estimated by the Gaussian error propagation method [18,19]:

$$\Delta R_i = \sqrt{\left(\frac{C_i}{A}\right)^2 \times \Delta q^2 + \left(\frac{q \times C_i}{A^2}\right)^2 \times \Delta A^2 + \left(\frac{q}{A}\right) \times \Delta C_i} \tag{2}$$

where Δ represents uncertainty of each parameter within a 95% confidence interval.

DATA INTERPRETATION

Far from equilibrium, the leaching process of fixated FGD material in acidic environments is influenced by two parallel surface chemical reactions; i.e., hydration and the proton-promoted reaction [20]. Therefore, the overall leaching rate of a specific element i is given by:

$$R_i = R_{i,H_2O} + R_{i,H} = R_{i,H_2O} + k_{i,H}(C_H^{surface})^j \tag{3}$$

where R_{i,H_2O} shows the intrinsic kinetics of the hydration reaction and $R_{i,H}$ is the rate due to proton-promoted leaching process; $k_{i,H}$ is the rate constant of the proton-promoted reaction; $C_H^{surface}$ is the concentration of surface-adsorbed protons (mole cm^{-2}) which is determined analytically by alkalimetric titration [21]; exponent *j* represents the order of the reaction. The overall leaching rate is controlled by the fastest reaction. According to surface complex formation equilibria and semi-empirical relations, $C_H^{surface}$ is shown to be nonlinearly related to $[H^+]_{surface}$, the proton concentration in the diffusion boundary layer on the water-solid interface (mole L^{-1}) [20,22,23]:

$$C_H^{surface} \propto [H^+]_{surface}^m$$

Therefore, the empirical rate law of the proton-promoted leaching process is shown as

$$R_{i,H} = k'_{i,H} [H^+]_{surface}^n \quad (4)$$

where n is equal to the product of *j* and *m*.

The theory of mass transfer in the vicinity of a rotating disk [24,25,26] can be applied to determine $[H^+]_{surface}$. By solving the convective diffusion equation [25] with corrected Schmidt number [26], the mass flux of reactant, i.e., proton, from the bulk solution to the disk surface, J (e.g., mole dm^{-2} sec^{-1}), is given by:

$$J = \frac{0.62048 Sc^{-2/3} \sqrt{\upsilon\omega}}{1 + 0.2980 Sc^{-1/3} + 0.1451 Sc^{-2/3}} ([H^+]_{Bulk} - [H^+]_{Surface}) \quad (5)$$

where k_d is transport rate constant (e.g., dm sec^{-1}); *Sc* is the Schmidt number (e.g., υ/D); υ is kinematic viscosity (e.g., dm^2 sec^{-1}); *D* is diffusion coefficient (e.g., dm^2 sec^{-1}); $[H^+]_{Bulk}$ is the concentration of proton in the bulk solution (e.g., mole L^{-1}); and ω is angular velocity (e.g., rad sec^{-1}). If the leaching process is limited by rate of mass transport, all proton molecules approaching the surface react spontaneously; therefore, $[H^+]_{Surface}$ can be assumed to be zero. In such a case, the leaching rate is equal to the transport rate of protons and eq. 4 is not applicable. $R_{i,H}$ is determined by:

$$J = \frac{0.62048 Sc^{-2/3} \sqrt{\upsilon\omega}}{1 + 0.2980 Sc^{-1/3} + 0.1451 Sc^{-2/3}} [H^+]_{Bulk} \quad (6)$$

Equation 6 indicates the magnitude of $R_{i,H}$ is proportional to the square root of the angular velocity at a fixed $[H^+]_{bulk}$ value.

If the leaching process is limited by the kinetics of the surface reaction, $R_{i,H}$ is independent of the mass flux of protons and therefore independent of the rotating speed. In such a case, the concentration of protons in the solution is assumed to be constant [25,27] and the rate of the leaching process is determined by:

$$R_{i,H} = k'_{i,H} [H^+]_{bulk}^n \quad (7)$$

If the rate of leaching is controlled by both mass transport and reaction kinetics, the boundary condition is more complicated and is discussed by Levich [25].

RESULTS AND DISCUSSION

Characteristics of the leaching process

Table 1 shows the XRD diffraction results for the constituents of fixated FGD material (i.e., lime, filter cake, and fly ash) and fixated FGD material samples before and after the leaching process had been conducted. Lime (CaO) and portlandite ($Ca(OH)_2$) are the main mineral phases found in the additional lime. The mineral composition of filter cake is dominated by hannebachite ($CaSO_3 \bullet 0.5H_2O$). The mineral phases of fly ash are more complicated. Alluminosilicates (i.e., mullite ($Al_6Si_2O_{13}$) and sillimanite (Al_2SiO_5)), iron oxides (i.e., magnetite (Fe_3O_4), hematite (Fe_2O_3)), and quartz (SiO_2) are the observed crystalline minerals. Except lime and portlandite, the fixated FGD material is composed of the minerals observed in those constituents. In addition, a secondary mineral, ettringite ($Ca_6Al_2(SO_4)_3(OH)_{12} \bullet 26H_2O$), was also found. After leaching, there was a loss of ettringite and hannebachite indicating these solids likely control the leaching process.

Figure 1 presents the mass flux profiles of Ca and S during the leaching process under the leaching condition of pH 2.2 and angular velocity of 60 rpm. Additional experiments were performed at higher pH values and different rotating speeds (data not shown). The mass flux of each selected element was calculated by:

$$q = C_{i,eff} \times Q \tag{9}$$

where $C_{i,eff}$ is effluent concentration of element i (e.g., μmole L^{-1}), Q is flow rate of leachant solution flow through the reactor (e.g., L min^{-1}). The mass fluxes of different elements at different leaching conditions exhibit a similar pattern; i.e., a rapid release at the early stage of the leaching process followed by an exponential decrease.

The observed transient is possibly the result of: (1) The existence of ultra-fine particles created naturally or from the surfacing procedure when the samples were prepared [28]. (2) A higher initial density of active sites. The Monte Carlo simulation model [29] shows the mole fractions of more active sites; such as adatom, ledge, and kink sites, are higher on the initial surface than on the steady-state surface. (3) The presence, and subsequent depletion, of more soluble mineral phases.

Transport versus reaction control

Table 2 shows the leaching rates of Ca, S, Al, Si, Fe, and Mg at pH2.2 with different rotating speeds. As can been seen, the increase of rotating speeds did not increase the leaching rate of all selected elements in acidic leaching conditions. A similar independent relationship of leaching rates and rotating speed was also found at pH 5.0 (data not shown). The observation indicates (1)

the change of hydrodynamics of the system has no effect on the leaching kinetics of fixated FGD material for all selected elements; therefore, the surface reaction mechanism controls the leaching kinetics; and (2) the surface concentration of proton equals the proton concentration in the bulk solution [25,27]. Any molecules that were detached from the surface were transported immediately into the bulk of the solution; therefore there is no accumulation of leached molecules on the surface and the interaction between leached elements and the surface can be ignored.

Effect of pH on the leaching kinetics

For surface-controlled leaching kinetics, eq.7 can used to express the pH effect on the leaching kinetics. Table 3 shows the leaching rates of selected elements at different acidic leaching conditions. The leaching rates of selected elements were constant at pH 6.8 and 5 indicating the overall leaching kinetics were controlled by an intrinsic hydration mechanism at near neutral pH conditions. When pH was below 3.7 (5.0 for Mg and Fe), leaching rates started increasing indicating the proton-promoted leaching process was dominating. Therefore, the overall leaching rate law of each element can be determined by attempting the linear regression at the ascending part of the logarithmic plot. The overall leaching rate (μmole cm^{-2} min^{-1}) can be written as:

$$R_i = R_{i,H_2O} + k'_{i,H} a_H^n \qquad (10)$$

where $k'_{i,H}$ is the rate constant (μmole cm^{-2} min^{-1}) and a_H is proton activity (dimensionless). Regression results are summarized in table 4. It is found that the reaction orders are very close to 0.5 and 0.75 for divalent ions; such as Ca, S, and Mg, and trivalent ions; i.e., Al and Fe, respectively. The mathematical model indicates the leaching rates of divalent and trivalent cations increase 3.2 and 5.2 times, respectively, when pH decreases 1 unit.

CONCLUSIONS

The leaching process of fixated FGD material conducted in a flow-through-rotating disk system shows an independent relationship of leaching kinetics on hydrodynamic condition suggesting the leaching process is controlled by a surface reaction mechanism over the pH range tested in this study, from pH2.2 to pH6.8. Therefore, the leaching rate, R_i, of a selected element can be written as eq.10:

$$R_i = R_{i,H_2O} + k'_{i,H} a_H^n$$

The regression results obtained from the plot of $\log R_i$ as a function of pH establishes a complete mathematic model describing the effect of pH on the release of the selected elements. The model suggests the leaching rates of divalent and trivalent cations increase 3.2 and 5.2 times, respectively, when pH decreases 1 unit.

REFERENCES

[1] Armesto, L. and Merino, J.L., Fuel, 1999, 78: p.613.

[2] Lecuyer, I., Bicocchi, S., Ausset, P., and Lefevre, R., Waste Management & Research, 1996, 14, p.15.

[3] Chen, X., Wolfe, W. E., Hargraves, and Malcolm, D., Fuel, 1997, 76, p.755.

[4] Chen, L., Dick, W. A., Nelson, S., Environmental Pollution, 2001, 114, p.161.

[5] Chun, S., Nishiyama, M., Matsumoto, S., Environmental Pollution, 2001, 114, p.453.

[6] Clark, R.B., Zeto, S.K., Ritchey, D., and Baligar, V.C., Fuel, 1997, 8, p.771.

[7] Crews, J.T., Dick, W.A., Environmental Pollution, 1998, 103, p.51.

[8] Stehouwer, R.C., Sutton, P., Dick, W. A., Soil Science, 1996, 161, p.562.

[9] Laperche, V., Traina, S.J, J. Environ. Qual., 1999, 28, p.1733.

[10] Rudisell, M.T., Struart, B.J., Novak, G., Payne, H., Togni, C.S., Fuel, 2001, 80, p.837.

[11] Lamminen, M., Wood, J., Walker, H.W., Chin, Y., He, Y., Traina, S.J., J. Environ. Qual., 2001, 30, p.1371.

[12] Payette, R. M., Wolfe, W.E., Beeghly, J., Fuel, 1997, 76, p.749.

[13] Butalia, Tarunjit S., Wolfe, William E., Fuel, 1998, 78, p.149.

[14] Ann,C., Mitsch,W. J., Wolfe, W. E., Wat. Res., 2001, 35, p.663.

[15] Solem-Tishmack, J.K., McCarthy, G..J., Cement and Concrete Research, 1995, 25, p.658.

[16] Teixeira, E.C., Samama, J., Brun, A, Environmental Technology, 1992, 13, p.1187.

[17] Kim, A.G., Proc., 15th International American Coal Ash Association Symposium on management & use of coal combustion products (CCPs). 2003, St. Petersburg, Florida.

[18] Barrante, J.R., Applied Methamatics for Physical Chemistry, Prentice-Hall Inc.: N.J. 1974.

[19] Cama, J., Ganor, J., Lasaga, C.A., Geochi. et Cosmochi. Acta 2000, 64, p.2701.

[20] W. Stumm, Chemistry of the solid-water interface, John Wiley and Sons, Inc., New York, 1992

[21] Furrer, G. and Stumm, W., Geochi. et Cosmochi. Acta,1986, p.1847.

[22] Stillings, L.L., Brantley, S.L., Machesky, M.L., Geochi. et Cosmochi. Acta, 1995, 59, p.1473.

[23] Lund, K., Fogler, H.S., McCune C.C., Chemical Engineering Science, 1973, 28, p.691.

[24] D.P. Gregory and A.C. Riddiford, J. Chem. Soc., 1956, p. 3756.

[25] Veniamin G. Levich, Physicochemical Hydrodynamics, Presentice-Hall, Inc., 1962, pp.60-78.

[26] Newman, J., J. Phys. Chem., 1966, 70, p.1327.

[27] Stone, A.T., and Morgan, J.J. In Aquatic Chemical Kinetics, (Ed Stumm, W.), John Wiley and Sons, Inc, New York, 1990, pp. 1-41.

[28]Samson, S. and Eggleston, C., *Environ. Sci, Technol.* 1998, 32, p.2870.

[29] Wehrli, B., J. Colloid and Interface Science, 1989, 132, p.230.

Table 1. XRD diffraction results for the constituents of fixated FGD and fixated FGD material samples before and after the leaching process had been conducted.

	lime	filter cake	fly ash	fixated FGD material	
				before leaching	after leaching
lime	●				
portlandite	●	●			
hannebachite		●		●	
mullite			●	●	●
sillimanite			●	●	●
magnetite			●	●	●
hematite			●	●	●
quartz			●	●	●
ettringite				●	

Table 2. Leaching rates of selected elements at different rotating speeds under leaching condition of pH2.2

Rotating speed (rpm)	Ca^{1}	S^{1}	Al^{1}	Si^{1}	Fe^{1}	Mg^{1}
6	11.5±0.7	7.7±0.4	1.0±0.1	0.84±0.06	0.21±0.02	0.39±0.03
30	11.4±0.8	8±1	1.1±0.1	0.8±0.1	0.22±0.02	0.39±0.03
60	13±2	8.9±0.7	1.3±0.1	1.00±0.09	0.26±0.02	0.45±0.04
90	9±1	5.5±0.8	0.9±0.1	0.7±0.1	0.16±0.03	0.25±0.09

[1] unit: μmole m^{-2} min^{-1}

Table 3. Leaching rates of selected elements at different acidic leaching conditions at rotating speed of 60 rpm

pH	Ca^{1}	S^{1}	Al^{1}	Si^{1}	Fe^{1}	Mg^{1}
6.8[2]	1.4±0.2	0.7±0.1	0.09±0.01	0.12±0.02	0.0014±0.0005	0.010±0.002
	1.1±0.1	0.6±0.07	0.08±0.01	0.13±0.02	0.0016±0.0005	0.007±0.001
5.0	1.5±0.2	0.7±0.2	0.10±0.02	0.2±0.1	0.002±0.002	0.012±0.006
3.7	2.4±0.4	1.3±0.2	0.10±0.02	0.22±0.05	0.015±0.004	0.06±0.03
2.9	6±1	3.8±0.8	0.38±0.06	0.47±0.01	0.08±0.01	0.18±0.03
2.2	13±2	8.9±0.7	1.3±0.1	1.00±0.09	0.26±0.02	0.45±0.04

[1] unit: μmole m^{-2} min^{-1}

[2] duplicate data has been shown

Table 4. Numerical results of pH effect on selected elements

pH of solution	Leaching Rate (μmole cm^{-2} min^{-1})					
	Ca^{2}	S^{2}	Al^{2}	Si^{2}	Mg^{3}	Fe^{3}
2.2	13±2	9±1	1.3±0.2	1.0±0.1	0.45±0.06	0.26±0.04
2.9	6±1	3.8±0.8	0.38±0.06	0.47±0.09	0.18±0.03	0.08±0.02
3.7	2.4±0.4	1.3±0.2	0.10±0.02	0.22±0.05	0.06±0.03	0.015±0.004
5.0	1.7±0.2	0.7±0.2	0.10±0.02	0.2±0.1	0.013±0.006	0.002±0.002
6.8[1]	1.4±0.2 1.1±0.1	0.8±0.1 0.60±0.07	0.09±0.01 0.08±0.01	0.13±0.02 0.12±0.02	0.010±0.002 0.007±0.0008	0.0016±0.0005 0.0014±0.0005
R_{H2O} (μmole cm^{-2} min^{-1})	1.4±0.3	0.7±0.2	0.9±0.3	0.2±0.1	0.01±0.007	0.0015±0.0006
k'_H (μmole cm^{-2} min^{-1})	166.3	155.3	55.8	9.6	7.7	13.1
n	0.50	0.55	0.73	0.44	0.56	0.76
r^2	0.9997	0.9992	0.9997	0.998	0.998	0.994

1 Duplicate data is shown
2 Regression ranges from pH3.7 to 2.2
3.Regression ranges from pH5.0 to 2.2

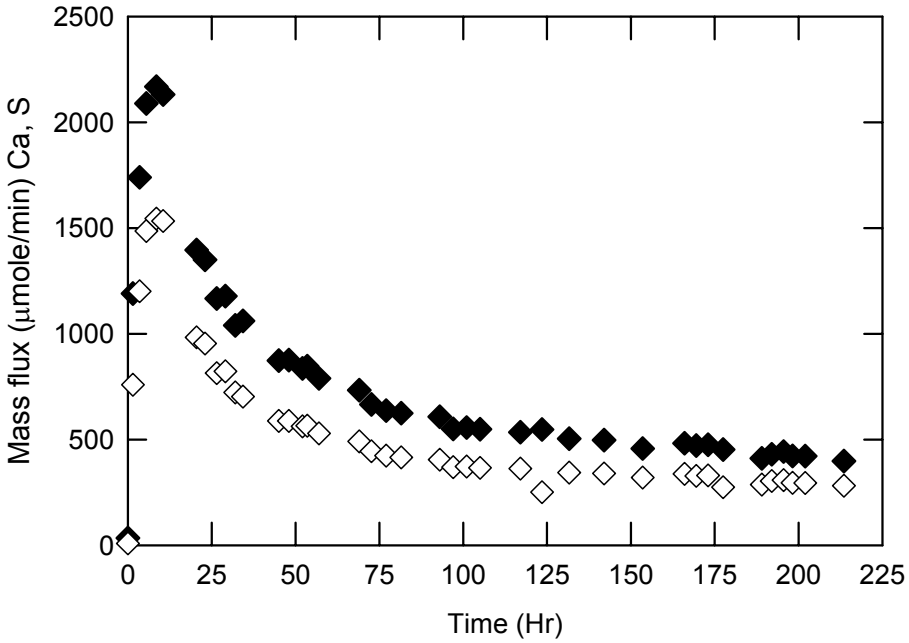

Figure 1. Mass flux profiles of selected elements over the leaching process under the leaching condition of pH 2.2 and angular velocity of 60 rpm. ◆ Ca; ◇ S